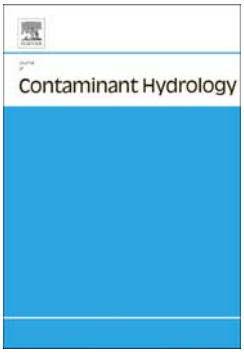

Enhanced Retention of Bacteria by TiO_2 Nanoparticles in Saturated Porous Media

Guillermina J. Gentile, María M. Fidalgo de Cortalezzi

PII: S0169-7722(16)30077-8
DOI: doi: 10.1016/j.jconhyd.2016.05.004
Reference: CONHYD 3219

To appear in: *Journal of Contaminant Hydrology*

Received date: 16 February 2016
Revised date: 11 May 2016
Accepted date: 22 May 2016

Please cite this article as: Gentile, Guillermina J., Fidalgo de Cortalezzi, María M., Enhanced Retention of Bacteria by TiO_2 Nanoparticles in Saturated Porous Media, *Journal of Contaminant Hydrology* (2016), doi: 10.1016/j.jconhyd.2016.05.004

Enhanced Retention of Bacteria by TiO_2 Nanoparticles in Saturated Porous Media

Guillermina J. Gentile[a], María M. Fidalgo de Cortalezzi[b,*]

[a] Department of Chemical Engineering, Instituto Tecnológico de Buenos Aires, Av. Eduardo Madero 399, 1106 Buenos Aires, Argentina. E-mail address: ggentile@itba.edu.ar

[b] Department of Civil and Environmental Engineering, University of Missouri, Columbia MO 65211, US. E-mail address: fidalgom@missouri.edu

* Corresponding author. Tel: +1 573 884 6777

Key words: Bacteria, TiO_2 nanoparticle transport in porous media. Cotransport. DLVO.

Abstract: The simultaneous transport of TiO_2 nanoparticles and bacteria *Pseudomonas aeruginosa* in saturated porous media was investigated. Nanoparticle and bacterium size and surface charge were measured as a function of electrolyte concentration. Sand column breakthrough curves were obtained for single and combined suspensions, at four different ionic strengths. DLVO and classical filtration theories were employed to model the interactions between particles and between particles and sand grains. Attachment of TiO_2 to the sand was explained by electrostatic forces and these nanoparticles acted as bonds between the bacteria and the sand, leading to retention. Presence of TiO_2 significantly increased the retention of bacteria in the sand bed, but microorganisms were released when nanomaterial influx ceased. The inclusion of nanomaterials in saturated porous media may have implications for the design and operation of sand filters in water treatment.

Nomenclature

a_b: radius of bacterium (m)

a_T: radius of TiO_2 (primary aggregate) (m)

A: Hamaker constant (J)

A_{bwb}: Hamaker constant of bacterium in water (J)

A_{bwq}: combined Hamaker constant of bacterium and quartz sand in water (J)

A_{Twb}: combined Hamaker constant of TiO_2 and bacterium in water (J)

A_{Twq}: combined Hamaker constant of TiO_2 and quartz sand in water (J)

A_{TwT}: Hamaker constant of TiO_2 in water (J)

C: suspended particle concentration in classical filtration theory

C_j: ion concentration (mol dm^{-3})

d_c: average diameter of the collector (m)

e: electron charge (C)

f: porosity

h: separation between surfaces (m)

k: Boltzmann constant (J K^{-1})

k_d: particle deposition rate coefficient (s^{-1})

L: bed length (m)

n_∞: bulk number of ions (ions m^{-3})

T: temperature (K)

U: Darcy velocity (m s^{-1})

V_{EDL}: electrical double layer interaction potential energy (J)

V_{TOTAL}: total interaction potential energy (J)

V_{vdW}: retarded van der Waals interaction potential energy (J)

z: valence of symmetrical (z-z) electrolyte

z_j: valence of ion j including sign of charge

α_c: clean-bed collision efficiency factor

γ: reduced surface potential

γ_b: bacterium reduced surface potential

γ_q: quartz sand reduced surface potential

γ_T: TiO_2 reduced surface potential

ζ: zeta potential (V)

η_0: single-collector efficiency

κ: Debye-Hückel reciprocal length (m^{-1})

λ: characteristic wavelength of the interaction (m)

φ: electrical surface potential (V)

1. Introduction

Groundwater contamination by pathogenic organisms is an important concern due to overgrowing populations with limited access to sanitation and safe drinking water. Urban population growth and higher demands on agricultural yield to feed an increasing number of people would eventually lead to detrimental effects on groundwater quality (Fidalgo de Cortalezzi et al., 2014; Smith Jr and Perdek, 2004). The World Health Organization (WHO) identified inadequate drinking water, sanitation and hygiene as responsible for 842,000 diarrheal disease deaths per year (WHO, 2014).

The transport and retention of microorganisms and colloids in porous media plays a key role in several natural processes and it is intimately related to sand filtration systems in water treatments (Harvey and Garabedian, 1991; McCarthy and Zachara, 1989; Ryan and Elimelech,

1996; Tufenkji and Elimelech, 2003; Tufenkji et al., 2002). Knowledge on bacteria transport through saturated porous media is fundamental to design bioremediation schemes and to evaluate the transport of pollutants associated to this kind of organisms (Steffan et al., 1999; Tufenkji, 2007).

Industrial manufacturing of nanomaterials has continually increased since the last decades of the 20th Century and is expected to follow this trend as they are used in pigments, absorbents, sunscreens, wastewater treatment compounds and catalysts (Bottero et al., 2015; Robichaud et al., 2009). The release of these materials to natural soils and waters, to some degree, is therefore unavoidable, and understanding their environmental impact have become even more relevant (Biswas and Wu, 2005; Boncagni et al., 2009; Tripathi et al., 2012; Xiao and Wiesner, 2013). Particularly, TiO_2 nanoparticles are highly relevant due to their widespread use (Boncagni et al., 2009; Bottero et al., 2015; Robichaud et al., 2009). At present, production of TiO_2 is around 88,000 ton/year (Bottero et al., 2015). Nanoparticles properties derive not only from their chemical structure, but also from their high surface area, small size, surface chemistry and electrical properties. These conditions may be altered when dispersed in natural environments (Boncagni et al., 2009; Chen and Mao, 2007; Indris et al., 2005; Klaine et al., 2008; Murdock et al., 2008). As much as their fate and transport in porous media is affected by the conditions in waters, other species will also be affected by their presence. Nanomaterials have shown a strong tendency to adsorb on biological surfaces (Chowdhury et al., 2012; Horst et al., 2010; Jucker et al., 1997; Schwegmann et al., 2013). Therefore, we can expect the combined transport of nanomaterials and microorganisms (bacteria, viruses, etc.) to be altered by this interplay.

Transport of microorganisms and transport of nanoparticles have been investigated using columns packed with glass beads, quartz sand and natural soils (Tufenkji, 2007). Studies so far concentrated on microorganism transport by itself, or nanomaterial mobility under the presence

of bacteria-modified porous media given by previous growth of biofilm or EPS-coated collectors, and showed that mobility of nanoparticles can be modified by the presence of bacteria. Nevertheless, we also expect the transport of microorganisms to be affected by the nanomaterials in saturated porous media.

The objective of the present work is advance our knowledge of bacteria transport in saturated porous media and to establish the effects of nanoparticles in the water flux, by investigating the interactions and simultaneous breakthrough for both species. To the best of our knowledge, this approach is the first with this type of nanoparticles and will contribute to the understanding of microorganisms' retention in soils and waters. We investigated the transport of *Pseudomonas aeruginosa* and P25 TiO_2 nanoparticles in saturated sand columns. Bacteria and nanomaterials were characterized with respect to size and surface charge. DLVO theory of colloidal stability, classical filtration theory and correlation equations were applied for data analysis (Derjaguin and Landau, 1941; Rajagopalan and Tien, 1976; Rajagopalan et al., 1982; Tufenkji and Elimelech, 2003; Verwey and Overbeek, 1955; Yao et al., 1971).

2. Materials and methods

The initial stock of bacteria *Pseudomonas aeruginosa* (ATCC 15692-B2) was kindly provided by Cátedra de Virología, Facultad de Farmacia y Bioquímica, Universidad de Buenos Aires. Aeroxide TiO_2 P25 nanoparticles were supplied by Evonik Degussa Corporation, NJ, USA. P25 is hydrophilic fumed TiO_2, mixture of rutile and anatase, with an average primary particle size of 21 nm, as reported by the manufacturer. Type I water (resistivity 18 MΩ.cm) and reagent grade NaCl (Anedra, Argentina) were used in all experiments. Nutrient broth (Britania, Argentina) for *P. aeruginosa* was prepared mixing 8 g in 1 L of water. Nutrient agar for Petri dishes was

prepared mixing 8 g of nutrient broth, 8 g of NaCl and 15 g of agar-agar technical for microbiology (Merck, Germany) in 1 L of water. Solutions and materials were sterilized by autoclaving at 121ºC for 20 minutes.

Multiplication and purification of bacteria were conducted as follows. First, the bacteria were incubated in nutrient broth for 24 hours at 37ºC placed on an orbital shaker at 120 rpm. The suspension was then centrifuged at 5800 xg for 15 minutes and the supernatant discarded. The pellet was resuspended in 10 mL of the desired solvent (water, 1 mM, 10 mM, or 100 mM NaCl) and centrifuged at 5800 xg for 15 minutes. This procedure was repeated twice. The final stock suspension was kept at 4ºC overnight prior to use (Schinner et al., 2010).

TiO_2 and bacteria particles were characterized with respect to size and zeta potential, at all ionic strengths, using a Zetasizer Nano ZS (Malvern, UK) at 21ºC. Size was determined by Dynamic Light Scattering (DLS) using number-weighted distribution. Large particles scatter more light than small particles because the intensity of scattering of a particle is proportional to the sixth power of its diameter (Rayleigh's approximation) (Malvern, 2007). Therefore, a large particle will produce a significant larger response than a small particle in the intensity-weighted distribution. However, as aggregation processes depend on particle number, when considering changes due to particle-particle and particle-collector attachment, number-weight distributions were considered more relevant than intensity-weight. Electrophoretic mobility of the particles was first measured by laser Doppler velocimetry and phase analysis light scattering, and then converted to zeta potential using the Smoluchowski equation as described elsewhere (Romanello and Fidalgo de Cortalezzi, 2013).

Ottawa No. 12 Flint silica sand (U.S. Silica Company, Berkeley Springs, WV), was used as model bed sediment in the laboratory column experiments. Prior to column packing, the sand was washed with constant agitation according to the following sequence: deionized water, HCl

solution (pH 3), deionized water, NaOH solution (pH 10), $NaHCO_3$ solution, deionized water (Packman et al., 2000). It was dried at 105ºC, and autoclaved at 121ºC for 20 minutes. Sand composition was analyzed by X-ray diffraction (XRD) (diffractometer PW 1730/10, Cu anode, 40 kV, 20 mA) confirming it was 100% quartz and determining Krumbein's roundness 0.7 and Rittenhouse sphericity 0.87. Sieve analysis indicated d_{50} of 529 μm by mass (Ren and Packman, 2002).

2.1. Column experiments

Column experiments were performed using a chromatography glass column with adjustable end pieces (Omnifit, Cambridge, UK) and internal diameter of 25 mm. The column was packed with silica sand under agitation and with a considerable height of water to avoid layering and bubbles of air (Schinner et al., 2010) and then Type I water was circulated until the electrical conductivity was close to zero. The length of the sand bed was 5 cm for all experiments. The effective porosity was determined from a tracer (NaCl) breakthrough curve and modeled with the aid of the software "CXTFIX21 (U.S. Salinity Laboratory Agricultural Research Service, U.S. Department of Agriculture, Riverside, California) as described elsewhere (Ren et al., 2000). Afterwards, solution of desired ionic strength was pumped for 20 minutes to stabilize the sand prior injection of nanoparticles or microorganisms.

2.2. Transport and breakthrough curves

Flow rate was constant and set at 2.8 mL/min. For the single particle transport study, 5 PV (pore volumes) of the suspension with TiO_2 or *Pseudomonas aeruginosa* at the desired ionic strength were pumped, followed by 3 PV of background solution. For the combined transport of both

bacteria and TiO_2, 4 PV of *P. aeruginosa* suspension with the desired ionic strength were pumped, followed by 3 PV of *P. aeruginosa* and TiO_2 suspension with the same ionic strength and then 3 PV of the *P. aeruginosa* suspension. In both cases, effluent samples were collected every 0.3 PV.

Breakthrough curves were obtained from a variety of incoming concentrations and ionic strength levels, presented in Table 1, representative of natural waters (Chowdhury et al., 2012). The feed concentration of bacteria in the suspensions was between $4x10^4$ and $8x10^6$ CFU/mL, while TiO_2 concentration varied between 30 and 100 ppm. Each experiment was repeated at least six times for TiO_2, four times for bacteria and three times for combined TiO_2 and *P. aeruginosa* transport, at each ionic strength. The working pH was between 5.2 and 5.8; it was measured and monitored but not adjusted since no significant change was evidenced during the experiments.

During the transport experiments bacteria were not expected to multiply since they were not in the optimum conditions, (absence of nutrients, low temperature), and the time of each run did not exceed 45 minutes. Furthermore, bacteria were harvested at the end of the logarithmic phase, minimizing the potential for cell numbers to increase (Vasiliadou and Chrysikopoulos, 2011).

For the single particle experiments, influent and effluent particle concentrations were measured by UV absorbance using a UV-Vis spectrophotometer (Shimadzu UV 1650 PC) at 325 nm for TiO_2 and at 262 nm for *P. aeruginosa* (wavelengths were determined from the peak of the individual adsorption spectra).

For the combined transport of *P. aeruginosa* and TiO_2, various techniques were used to minimize quantification errors due to particle interference (Table 1). For the first part of the experiment, when only the suspension of *P. aeruginosa* was pumped through the column, the bacteria concentration was detected photometrically at 262 nm. When both particles were present

in the feed, qPCR was employed to quantify bacteria, while TiO_2 nanoparticles were analyzed by microwave digestion followed by a spectrophotometric method.

qPCR was performed using CFX96 (Bio-Rad, USA) and PowerWater DNA isolation kit (Mo Bio Laboratories Inc., CA, USA) to extract the DNA of the bacteria. A portion of the gene encoding 16S rRNA of *P. aeruginosa* chromosome was amplified. Quantification was made by absolute PCR using SyBr-Green (Bio-Rad, USA).

To determine the TiO_2 concentration, each sample was treated as follows: 3 mL of sample was mixed with 3 mL of H_2SO_4 (18 M) and 0.23 g of $(NH_4)_2SO_4$ and then digested in a MARS 5 microwave reaction system (CEM, NC, USA). Afterwards, samples were centrifuged at 3000 rpm for 15 min to remove decanted organic matter, 1 ml of H_2O_2 (30%) added and water up to 10 mL. Finally, sample absorbance was measured at 410 nm (Shimadzu UV 1650 PC).

2.3. DLVO theory

DLVO theory was used to model the attachment of bacterium and TiO_2 to sand grains and the aggregation of both particles. TiO_2 nanoparticles and bacteria were considered spheres with diameters equal to their hydrodynamic diameters. In the case of the rod-shaped bacterium, this dimension represents an equivalent diameter that can be related to the average of the two dimensions of the short rod. Sand was regarded as an infinite plate.

Interactions between sphere and plate (TiO_2 and sand, bacterium and sand) were calculated using the following expressions for van der Waals (Eq. 1) and electrostatic double layer (Eq. 2) interactions (Gregory, 1975; Gregory, 1981):

$$V_{vdW} = -\frac{A_{iwq}\, a_i}{6\, h}\left[1 - \frac{5.32\, h}{\lambda}\ln\left(1 + \frac{\lambda}{5.32\, h}\right)\right] \qquad (1)$$

$$V_{EDL} = \frac{128\,\pi\,a_i\,n_\infty}{\kappa^2}\;k\,T\,\gamma_i\,\gamma_q\,exp(-\kappa h) \qquad (2)$$

where V_{vdW}: retarded van der Waals interaction potential energy (J), V_{EDL}: electrical double layer interaction potential energy (J), A_{iwq}: Hamaker constant for the particle (TiO_2 or bacterium) and quartz surface suspended in water (J), a_i: radius of the sphere (TiO_2 or bacterium) (primary aggregate) (m), h: separation (m), λ: characteristic wavelength of the interaction (assumed to be 100 nm), n_∞: bulk number of ions (ions m^{-3}), κ: Debye-Hückel reciprocal length (m^{-1}), k: Boltzmann constant (J K^{-1}), T: temperature (K), γ_i: reduced surface potential of the sphere (TiO_2 or bacterium), γ_q: reduced surface potential of the plate (quartz).

Interactions between two different spheres (TiO_2 and bacterium) were calculated using Eqs. 3 and 4 when $h \ll a_i$ (Gregory, 1975; Gregory, 1981):

$$V_{vdW} = -\frac{A_{Twb}\,a_T\,a_b}{6\,(a_T + a_b)\,h}\left[1 - \frac{5.32\,h}{\lambda}\,\ln\left(1 + \frac{\lambda}{5.32\,h}\right)\right] \qquad (3)$$

$$V_{EDL} = \frac{128\,\pi\,a_T\,a_b\,n_\infty}{(a_T + a_b)\,\kappa^2}\;k\,T\,\gamma_T\,\gamma_b\,exp(-\kappa h) \qquad (4)$$

where A_{Twb}: Hamaker constant for two spheres (TiO_2 and bacterium) in water (J); with the aid of Eqs. 5 and 6 (Elimelech et al., 1995):

$$\gamma_i = Tanh\,\frac{z\,e\,\varphi_i}{4\,k\,T} \qquad (5)$$

$$\kappa = 2.32 \times 10^9 \sqrt{\sum C_j \, z_j^2} \qquad (6)$$ in aqueous solutions at 25ºC

where z: valence of symmetrical (z-z) electrolyte, e: electron charge (C), φ_i: electrical surface potential (V) which cannot be determined and was replaced by ζ_i: zeta potential (V), C_j: ion concentration (mol dm^{-3}), z_j: valence of ion j including sign of charge.

For the case of two equal spheres of TiO_2 or bacteria Eqs. 3 and 4 were reduced to Eqs. 7 and 8 respectively:

$$V_{vdW} = -\frac{A_{iwi}\, a_i}{12\, h}\left[1 - \frac{5.32\, h}{\lambda}\ln\left(1 + \frac{\lambda}{5.32\, h}\right)\right] \qquad (7)$$

$$V_{EDL} = \frac{64\,\pi\, a_i\, n_\infty}{\kappa^2}\, k\, T\, \gamma_i^2\, exp(-\kappa h) \qquad (8)$$

where A_{iwi}: Hamaker constant of TiO_2 or bacterium in water (J).

DLVO theory considers the total interaction potential energy as the sum of both van der Waals and electrical double layer potential energies (Eq. 9):

$$V_{TOTAL} = V_{vdW} + V_{EDL} \qquad (9)$$

The Hamaker constants employed were calculated from data obtained in the literature (Chowdhury et al., 2011; Petosa et al., 2010; Redman et al., 2004; Schinner et al., 2010; Schwegmann et al., 2013): $A_{bwq} = 6.5\text{x}10^{-21}$ J, $A_{Twq} = 1\text{x}10^{-20}$ J, $A_{Twb} = 4.6\text{x}10^{-21}$ J, $A_{TwT} = 6\text{x}10^{-20}$ J, $A_{bwb} = 1.015\text{x}10^{-22}$ J. Zeta potential of quartz sand was obtained from literature (Redman et

al., 2004): -40 mV in water, -39 mV in NaCl 1 mM, -22 mV in NaCl 10 mM, -10 mV in NaCl 100 mM.

2.4. Sand bed removal

The attachment of TiO_2 and *Pseudomonas aeruginosa* to the porous bed was evaluated using the classical filtration equation (Eq. 10) as well as the particle deposition rate (Eq. 11) (Tufenkji and Elimelech, 2003; Yao et al., 1971):

$$\frac{dC}{dL} = -\frac{3}{2}\frac{1-f}{d_c}\,\alpha_c\,\eta_0\,C \qquad (10)$$

$$k_d = \frac{3}{2}\frac{1-f}{f\,d_c}\,U\,\alpha_c\eta_0 \qquad (11)$$

where C: suspended particle concentration, L: bed length (m), f: porosity, d_c: average diameter of the collector (m), α_c: clean-bed collision efficiency factor, η_0: single-collector efficiency, k_d: particle deposition rate coefficient, U: Darcy velocity (m s^{-1}).

The single-collector efficiency, considered to be the addition of Brownian diffusion, interception and gravitational sedimentation, was calculated using the Tufenkji-Elimelech equation (TEE) (Tufenkji and Elimelech, 2003), and is presented with further detail in the Supplementary Information. For the case of combined transport, a pseudo-collision efficiency factor was also calculated, considering the initial ("clean") collector to be the bacteria-modified sand particles, at the first stages of nanoparticle influx.

The required parameters for calculating the clean-bed collision efficiency factor, the single-collector efficiency and the particle deposition rate coefficient were calculated from our experimental data obtained during the transport of TiO_2 and *P. aeruginosa*.

3. Results and discussion

3.1. Characterization of *Pseudomonas aeruginosa* and TiO_2

The average particle size and zeta potential of the bacterium and TiO_2 were determined for a range of ionic strengths between deionized water and 100 mM, at pH 5.8 (Fig. 1).

P. aeruginosa is a coccobacillus bacterium, not a perfect sphere and then the hydrodynamic diameter obtained by Dynamic Light Scattering (DLS) does not reflect its real size, but accounts for an equivalent diameter that can be related to the average of the two dimensions of the short rod. Moreover, bacteria are not rigid but dynamic in size as they interact with the solvent in which they are suspended. Therefore, the calculated diameter indicates the apparent size taking into consideration attraction and association with water molecules and electrolytes.

The size of the bacterium remained relatively uniform under the different ionic strengths, between 898±45 nm and 1034±136 nm. Its equivalent diameter is in agreement with isolated bacterium sizes reported in the literature (Çetin et al., 1965) suggesting the absence of aggregation. In contrast, the hydrodynamic size of TiO_2 was significantly affected by the ionic strength. When suspended in pure water, TiO_2 was present as 109±23nm aggregates, in concordance with previous publications (Mandzy et al., 2005; Romanello and Fidalgo de Cortalezzi, 2013; Thio et al., 2011). TiO_2 rapidly aggregated in aqueous solutions, as a consequence of its reactivity and high surface area (Ben-Moshe et al., 2010). Furthermore, ionic

strength enhanced attachment efficiency resulting in increase of aggregate size, especially for ionic strengths over 1 mM, reaching sizes well over 1μm. The samples were subjected to slow mixing during preparation that caused first interactions and then contact of nanoparticles, which, in turn led to aggregation (Boncagni et al., 2009) and corresponded to the physical transport mechanisms of the classical aggregation theory (Stumm and Morgan, 1996).

At the working pH, *P. aeruginosa* was negatively charged while TiO_2 exhibited positive surface charge in agreement with the reported isoelectric point for the metal oxide of 6.7 (Boncagni et al., 2009; Kosmulski, 2002). Zeta potential of the bacterium varied from -39 to -14 mV and between 29 and 21 mV for TiO_2 with increasing ionic strength (DI water to 100 mM).

DLVO theory predicted repulsion between two bacterial particles for all the studied conditions (Fig. S1 in Supplementary Information), as it was confirmed experimentally.

As ionic strength was increased, larger TiO_2 aggregates were found, in accordance with DLVO modeling (Fig. S2 in Supplementary Information). Reduction in zeta potential and compression of the electrical double layer resulted in lower energy barriers at higher electrolyte concentrations, and for NaCl 100 mM only attractive forces between the particles were predicted.

3.2. Transport of TiO_2

P25 column experiments were conducted by pumping 5 PV of TiO_2 solution with the desired ionic strength (water, 1, 10 or 100 mM NaCl), followed by 3 PV of background solution.

Fig. 2 shows the breakthrough curves at each ionic of the four conditions of ionic strength (ultrapure water; 1, 10, 100 mM) and the three levels of influent nanoparticle concentration (30, 50 and 100 ppm). In all cases, tracer solution (NaCl) was circulated prior to transport experiment to determine column porosity and check sand packing, also shown in Fig. 2. A plateau was

reached for water and 1 mM ionic strength respectively (Fig. 2.a and b); but for higher ionic strengths (10 and 100 mM) a peak was reached and then concentration at outlet decreased (Fig. 2.c and d), which hints to an increasing removal efficiency.

Three different factors can be responsible for the retention of TiO_2 in the porous media. First, attraction forces between quartz sand and TiO_2 due to the difference in their surface charges (attachment to the clean bed). Second, electrolyte concentration that causes aggregation during the transport of TiO_2 rendering it more difficult for the particles to pass through the pores (straining). Third, attachment of TiO_2 to previously deposited particles due to the attraction forces among them as discussed above (attachment to the ripe bed).

Electrostatic forces take into account surface charge differences between the negative sand and the positive TiO_2. As nanoparticles were retained, the collector's surface became progressively heterogeneous, so some particles would deposit onto the original sand while others would collide with previously attached TiO_2. SEM images showing this heterogeneity are provided in Supplementary Information (Fig. S6-S11); the size of each aggregate and frequency on the surface diminishes seems to decrease from the top layers of sand to the deeper grains, indicating less influence of repulsive forces as well as less quantity of TiO_2 to remove due to further retention in the first centimeters of the porous bed. When particles were suspended in deionized water and repulsion was dominant, collector attachment resulted in a monotonic increase of effluent particle concentration (Fig. 2.a). As ionic strength was increased, the attachment efficiency between TiO_2 particles was also increased and the effluent particle concentration dropped (Fig. 2.b, c and d). Based on DLVO calculations (Fig. S2), repulsion will be present between TiO_2, except when suspended in 100 mM ionic strength. When particles are passing through the column, these dominant repulsion forces will lead to increasing effluent concentration with time (Johnson and Elimelech, 1995; Johnson et al., 1996). Besides, particles

will find less free surface on the collector due to previous deposition; which in turn will contribute to this effect.

The variation of TiO_2 concentration in the feed affected the effluent concentration in the absence of electrolyte (Fig. 2.a); making it higher at higher incoming concentration. A strong attachment between TiO_2 and sand was predicted by DLVO theory (Fig. S3 in Supplementary Information), and deposition was expected as long as there was free collector surface available. When the surface was more covered in nanoparticles, it created repulsion between this layer and new incoming TiO_2; DLVO modeling of TiO_2-TiO_2 interactions (Fig. S2 in Supplementary Information) showed a significant energy barrier. For the highest feed concentration (100 ppm), collectors were covered in nanoparticles sooner due to enhanced chances of collisions, which in turn prevented new deposition and effluent concentration augmented.

At 1 mM ionic strength, DLVO showed a moderate energy barrier (Fig. S2 in Supplementary Information) and the system was closer to its critical coagulation concentration (Boncagni et al., 2009), so increased attachment efficiency was attained and deposition resulted independent of particle concentration.

For the highest ionic strengths, TiO_2 easily aggregated and attachment to sand and previously deposited particles was a consequence of the high attachment efficiency and particle size growth, independent of feed concentration.

DLVO calculations for the interactions between TiO_2 particles and sand collectors (Fig. S3 in Supplementary Information) resulted in strong attractive but no repulsion forces due to the opposite sign of the surface charges. As ionic strength increased, the electrical double layer interactions tend to a zero value, diminishing their relative importance when compared to the van der Waals attraction.

The experiments showed that TiO_2 retention levels in saturated sand were independent of incoming concentration for moderate to high ionic strengths in this study (10 to 100 mM) (Fig. 2.c and d), but not for the lowest ionic strength (Fig. 2.a).

When increasing particle concentrations, greater elution of nanoparticles was observed in previous published work at low ionic strength (1 mM). In DI water, interactions between two particles of TiO_2 are not favorable, thus limiting further deposition onto the sand after the initial layer. Besides, surface coverage was increased with increasing concentration due to aggregate size; indicating that more nanoparticles covered the free surface faster. Thus, higher inlet concentration, resulted in higher elution, may be due to blocking that may lead to repulsion among deposited and suspended particles (Chowdhury et al., 2011). At low concentrations of TiO_2, attachment of nanoparticles onto quartz sand increased when increasing concentration of the suspended particles; however, at high concentrations, a different situation occurred, since the amount of attachment stabilized indicating that all the surface sites on the sand were already occupied and remnant TiO_2 will not be attached to the sand grains. This affinity between the sand and the TiO_2 is due to strong attractive forces as predicted by DLVO theory, producing the attachment of a great number of TiO_2 to the quartz (Wu and Cheng, 2016).

3.3. Transport of *Pseudomonas aeruginosa*

Pseudomonas aeruginosa transport experiments were conducted by pumping 5 PV of bacterial suspension with the desired ionic strength, followed by 3 PV of background solution. Breakthrough curves are shown in Fig. 3.

Surface charge of bacteria was always negative and therefore not expected to be significantly retained by the also negatively charged sand. However, as ionic strength increased, some retention was observed. This effect can be explained by DLVO theory (Fig. S4 in

Supplementary Information). For ionic strengths up to 10 mM, no net attracting forces were present and a high energy barrier was predicted. The energy barrier diminished as ionic strength increased because of the compression of the electrical double layer and of the reduction of the zeta potentials. For ionic strength of 100 mM, the energy barrier disappeared completely and the net forces were attractive, favoring attachment.

3.4. Combined transport of *Pseudomonas aeruginosa* and TiO_2

In the combined transport experiments, 4 PV of *Pseudomonas aeruginosa* suspension were first pumped through the sand bed with the desired ionic strength, followed by 3 PV of a suspension containing both *P. aeruginosa* and TiO_2, and finally 3 PV of the original suspension of *P. aeruginosa*.

Fig. 4 shows the breakthrough curves for *P. aeruginosa* in the presence of TiO_2. These concentrations were determined by qPCR. The detection limit was 24.1 CFU and the quantification limit was 241 CFU. Agarose gel electrophoresis was performed to corroborate the reaction products and the quality of the standard. Additionally, it was determined that the presence of TiO_2 nanoparticles did not generate inhibition of the polymerase chain reaction, through a control test using a standard corresponding to a DNA fragment of *Arabidopsis thaliana*.

The transport characteristics of the bacteria were highly modified by the presence of TiO_2. Retention in the sand bed was observed, in contrast to the bacteria flow observed in the single particle experiments. The quantity of bacteria retained was increased with ionic strength, probably as a consequence of the formation of large TiO_2-bacterium aggregates that clogged the pores (Chowdhury et al., 2012).

Fig. 4 shows that after reaching the initial plateau, effluent bacteria concentration suffered a sharp decrease coincident with the injection of TiO_2. This effect was important even for pure water suspensions and retention remained very high for the duration of the TiO_2 injection. After TiO_2 injection stopped, bacteria concentration at outlet showed an increasing trend indicating that the microorganisms were transported through the sand bed again. DLVO theory predicted the attachment between TiO_2 and bacteria due to the difference in surface charges (Fig. S5 in Supplementary Information), although non-DLVO Lewis acid-base interactions and hydrogen bonds could also be partially responsible for the increasing attachment efficiency (Jiang et al., 2013).

Fig. 5 shows the breakthrough curves for TiO_2 in the presence of bacteria. The breakthrough of TiO_2 only suspensions is shown for comparison. The retention of TiO_2 by the sand was highly increased by the presence of bacteria, probably due in part to the formation of larger aggregates of nanoparticles and bacteria. The first layer of TiO_2 attached to the sand was responsible for adhering incoming microorganisms, which can in turn attract new particles of TiO_2. This process continued as long as both kinds of particles were injected. It can also be seen that in both cases, with and without the presence of the bacteria, the concentration of TiO_2 at the outlet was modified by the ionic strength, showing an increase in retention with increasing ionic strength, as predicted by DLVO theory and discussed above. This last observation suggests that electrostatic repulsion, modulated by the electrolyte concentration, played a fundamental role in the retention of the nanomaterial. Moreover, it can be clearly observed that concentrations of bacteria and TiO_2 at outlet diminished when both of them were present together, compared to the case when only one of them was in the stream; this suggests attachment of TiO_2 to both bacteria and sand, causing retention of microorganisms due to heteroaggregation.

3.5. Sand bed removal

The average single-collector efficiency (η_0), clean-bed collision efficiency factor (α_c) and particle deposition rate coefficient (k_d) for TiO_2 and for *Pseudomonas aeruginosa* were calculated (Table S1 in Supplementary Information).

Efficiency factors for bacteria and TiO_2 attachment to the collectors gave higher values for increasing ionic strength, and thus increased retention in the porous bed, as confirmed in the laboratory experiences and in agreement with attachment controlled by classical DLVO interactions (Jucker et al., 1997; Jucker et al., 1998; Mitzel and Tufenkji, 2014).

Collision efficiency factors above unity are theoretically impossible, but those between 1 and 1.25 are not considered rare. Discrepancies between the actual shape of collectors and the perfect spheres considered in the TEE can cause these overestimated values, as well as the size of the TiO_2 particle employed which is subject to aggregation (Foppen et al., 2010). It is important to note however, that the TEE was derived based on experimental data and was widely validated and employed, offering valuable parameters to compare different situations. Moreover, high values of collision efficiency factors suggest coexistence of straining along with physicochemical filtration (Jaisi et al., 2008).

To compare the attachment of TiO_2 with and without concurrent flow of bacteria, a pseudo-collision efficiency factor was calculated (considering the individual plateau concentration for each particle obtained from the breakthrough curves in Fig. 5). These values were significantly higher (between 32 and 53%) than those found in the single particle experiment for all ionic strengths, hinting to a synergistic effect on the retention in the combined transport (Fig. 6).

4. Conclusions

In this work, we showed that P25 TiO_2 was retained by the quartz sand due to aggregation and electrostatic attraction leading to attachment. At low ionic strengths, the attachment to the sand grains was low but it increased over time when ionic strength augmented. Bacteria were transported through the porous media, with minimal retention; however, a completely different scenario arose when nanoparticles were present in the water matrix, and bacteria were retained up to 99.99%. A combination of straining due to heteroaggregation of bacteria and TiO_2 nanoparticles in the incoming suspension and a more favorable condition for removal given by a ripening effect in the sand bed due to previously deposited particles is responsible for the increased retention. Besides, electrostatic repulsion, controlled by ionic strength, played a fundamental role in the removal of the nanomaterial.

The transport of microorganisms in porous media (aquifers, sand filters) is an important issue in both natural and engineering systems. We have shown that the transport of bacteria in saturated porous media is severely hampered by the presence of TiO_2 nanoparticles. Inclusion of these nanoparticles in sand beds offers the possibility to design an effective barrier for microorganisms, as a preventing measure, as a drinking water filter enhancer, or as a mean for retention of active bacteria and biofilm growth during a bioremediation process within the boundaries of the contaminant plume. However, this addition of nanoparticles should be designed carefully, considering the potential consequences brought by the incorporation of nanoparticles in the system.; for example, the pulse-like influx of nanomaterials in natural environments (sand aquifers) may be responsible for potential hazardous high concentrations of bacteria in the groundwater due to release of previously retained organisms after the nanoparticle input stops.

References

Ben-Moshe, T., Dror, I. and Berkowitz, B., 2010. Transport of metal oxide nanoparticles in saturated porous media. Chemosphere, 81(3): 387-393.

Biswas, P. and Wu, C.Y., 2005. Nanoparticles and the environment. J. Air Waste Manage. Assoc., 55(6): 708-746.

Boncagni, N.T. et al., 2009. Exchange of TiO_2 nanoparticles between streams and streambeds. Environ. Sci. Technol., 43(20): 7699-7705.

Bottero, J.-Y. et al., 2015. Nanotechnology, global development in the frame of environmental risk forecasting. A necessity of interdisciplinary researches. C. R. Geosci., 347(1): 35-42.

Çetin, E.T., Töreci, K. and Anğ, Ö., 1965. Encapsulated *Pseudomonas aeruginosa* (*Pseudomonas aeruginosa mucosus*) strains. J. Bacteriol., 89(5): 1432-1433.

Chen, X. and Mao, S.S., 2007. Titanium dioxide nanomaterials: Synthesis, properties, modifications and applications. Chem. Rev., 107(7): 2891-2959.

Chowdhury, I., Cwiertny, D.M. and Walker, S.L., 2012. Combined factors influencing the aggregation and deposition of nano-TiO_2 in the presence of humic acid and bacteria. Environ. Sci. Technol., 46(13): 6968-6976.

Chowdhury, I., Hong, Y., Honda, R.J. and Walker, S.L., 2011. Mechanisms of TiO_2 nanoparticle transport in porous media: Role of solution chemistry, nanoparticle concentration, and flowrate. J. Colloid Interf. Sci., 360(2): 548-555.

Derjaguin, B. and Landau, L., 1941. Theory of the stability of strongly charged lyophobic sols and of the adhesion of strongly charged particles in solutions of electrolytes. Acta Physicochim. URSS, 14: 733-762.

Elimelech, M. et al., 1995. Particle, Deposition & Aggregation. Butterworth-Heinemann, Woburn.

Fidalgo de Cortalezzi, M.M. et al., 2014. Virus removal by iron oxide ceramic membranes. J. Environ. Chem. Eng., 2(3): 1831-1840.

Foppen, J.W., Lutterodt, G., Röling, W.F.M. and Uhlenbrook, S., 2010. Towards understanding inter-strain attachment variations of *Escherichia coli* during transport in saturated quartz sand. Water Res., 44(4): 1202-1212.

Gregory, J., 1975. Interaction of unequal double layers at constant charge. J. Colloid Interf. Sci., 51(1): 44-51.

Gregory, J., 1981. Approximate expressions for retarded van der Waals interaction. J. Colloid Interf. Sci., 83(1): 138-145.

Harvey, R.W. and Garabedian, S.P., 1991. Use of colloid filtration theory in modeling movement of bacteria through a contaminated sandy aquifer. Environ. Sci. Technol., 25(1): 178-185.

Horst, A.M. et al., 2010. Dispersion of TiO_2 nanoparticle agglomerates by *Pseudomonas aeruginosa*. Appl. Environ. Microbiol., 76(21): 7292-7298.

Indris, S. et al., 2005. Preparation by high-energy milling, characterization, and catalytic properties of nanocrystalline TiO_2. J. Phys. Chem. B, 109(49): 23274-23278.

Jaisi, D.P., Saleh, N.B., Blake, R.E. and Elimelech, M., 2008. Transport of Single-Walled Carbon Nanotubes in Porous Media: Filtration Mechanisms and Reversibility. Environ. Sci. Technol., 42(22): 8317-8323.

Jiang, X., Wang, X., Tong, M. and Kim, H., 2013. Initial transport and retention behaviors of ZnO nanoparticles in quartz sand porous media coated with *Escherichia coli* biofilm. Environ. Pollut., 174(0): 38-49.

Johnson, P.R. and Elimelech, M., 1995. Dynamics of Colloid Deposition in Porous Media: Blocking Based on Random Sequential Adsorption. Langmuir, 11(3): 801-812.

Johnson, P.R., Sun, N. and Elimelech, M., 1996. Colloid Transport in Geochemically Heterogeneous Porous Media: Modeling and Measurements. Environ. Sci. Technol., 30(11): 3284-3293.

Jucker, B.A., Harms, H., Hug, S.J. and Zehnder, A.J.B., 1997. Adsorption of bacterial surface polysaccharides on mineral oxides is mediated by hydrogen bonds. Colloids Surf., B, 9(6): 331-343.

Jucker, B.A., Harms, H. and Zehnder, A.J.B., 1998. Polymer interactions between five gram-negative bacteria and glass investigated using LPS micelles and vesicles as model systems. Colloids Surf., B, 11(1–2): 33-45.

Klaine, S.J. et al., 2008. Nanomaterials in the environment: Behavior, fate, bioavailability, and effects. Environ. Toxicol. Chem., 27(9): 1825-1851.

Kosmulski, M., 2002. The pH-Dependent Surface Charging and the Points of Zero Charge. J. Colloid Interf. Sci., 253(1): 77-87.

Malvern, 2007. Zetasizer Nano Series User Manual. Malvern Instruments Ltd., Worcestershire, UK.

Mandzy, N., Grulke, E. and Druffel, T., 2005. Breakage of TiO_2 agglomerates in electrostatically stabilized aqueous dispersions. Powder Technol., 160(2): 121-126.

McCarthy, J.F. and Zachara, J.M., 1989. Subsurface transport of contaminants. Mobile colloids in the subsurface environment may alter the transport of contaminants. Environ. Sci. Technol., 23(5): 496-502.

Mitzel, M.R. and Tufenkji, N., 2014. Transport of industrial PVP-stabilized silver nanoparticles in saturated quartz sand coated with *Pseudomonas aeruginosa* PAO1 biofilm of variable age. Environ. Sci. Technol., 48(5): 2715-23.

Murdock, R.C., Braydich-Stolle, L., Schrand, A.M., Schlager, J.J. and Hussain, S.M., 2008. Characterization of nanomaterial dispersion in solution prior to in vitro exposure using dynamic light scattering technique. Toxicol. Sci., 101(2): 239-253.

Packman, A.I., Brooks, N.H. and Morgan, J.J., 2000. Kaolinite exchange between a stream and streambed: Laboratory experiments and validation of a colloid transport model. Water Resour. Res., 36(8): 2363-2372.

Petosa, A.R., Jaisi, D.P., Quevedo, I.R., Elimelech, M. and Tufenkji, N., 2010. Aggregation and deposition of engineered nanomaterials in aquatic environments: Role of physicochemical interactions. Environ. Sci. Technol., 44(17): 6532-6549.

Rajagopalan, R. and Tien, C., 1976. Trajectory analysis of deep-bed filtration with the sphere-in-cell porous media model. AIChE J., 22(3): 523-533.

Rajagopalan, R., Tien, C., Pfeffer, R. and Tardos, G., 1982. Letters to the editor. AIChE J., 28: 871-872.

Redman, J.A., Walker, S.L. and Elimelech, M., 2004. Bacterial adhesion and transport in porous media: Role of the secondary energy minimum. Environ. Sci. Technol., 38(6): 1777-1785.

Ren, J. and Packman, A.I., 2002. Effects of background water composition on stream-subsurface exchange of submicron colloids. J. Environ. Eng., 128(7): 624-634.

Ren, J., Packman, A.I. and Welty, C., 2000. Correlation of colloid collision efficiency with hydraulic conductivity of silica sands. Water Resour. Res., 36(9): 2493-2500.

Robichaud, C.O., Uyar, A.E., Darby, M.R., Zucker, L.G. and Wiesner, M.R., 2009. Estimates of upper bounds and trends in nano-TiO_2 production as a basis for exposure assessment. Environ. Sci. Technol., 43(12): 4227-4233.

Romanello, M.B. and Fidalgo de Cortalezzi, M.M., 2013. An experimental study on the aggregation of TiO_2 nanoparticles under environmentally relevant conditions. Water Res., 47(12): 3887-3898.

Ryan, J.N. and Elimelech, M., 1996. Colloid mobilization and transport in groundwater. Colloids Surf., A, 107: 1-56.

Schinner, T. et al., 2010. Transport of selected bacterial pathogens in agricultural soil and quartz sand. Water Res., 44(4): 1182-1192.

Schwegmann, H., Ruppert, J. and Frimmel, F.H., 2013. Influence of the pH-value on the photocatalytic disinfection of bacteria with TiO_2 - Explanation by DLVO and XDLVO theory. Water Res., 47(4): 1503-1511.

Smith Jr, J.E. and Perdek, J.M., 2004. Assessment and management of watershed microbial contaminants. Crit. Rev. Environ. Sci. Tecnol., 34(2): 109-139.

Steffan, R.J., Sperry, K.L., Walsh, M.T., Vainberg, S. and Condee, C.W., 1999. Field-scale evaluation of in situ bioaugmentation for remediation of chlorinated solvents in groundwater. Environ. Sci. Technol., 33(16): 2771-2781.

Stumm, W. and Morgan, J.J., 1996. Aquatic Chemistry: Chemical Equilibria and Rates in Natural Waters. John Wiley, New York.

Thio, B.J.R., Zhou, D. and Keller, A.A., 2011. Influence of natural organic matter on the aggregation and deposition of titanium dioxide nanoparticles. J. Hazard. Mater., 189(1–2): 556-563.

Tripathi, S., Champagne, D. and Tufenkji, N., 2012. Transport behavior of selected nanoparticles with different surface coatings in granular porous media coated with *Pseudomonas aeruginosa* biofilm. Environ. Sci. Technol., 46(13): 6942-6949.

Tufenkji, N., 2007. Modeling microbial transport in porous media: Traditional approaches and recent developments. Adv. Water Resour., 30(6–7): 1455-1469.

Tufenkji, N. and Elimelech, M., 2003. Correlation equation for predicting single-collector efficiency in physicochemical filtration in saturated porous media. Environ. Sci. Technol., 38(2): 529-536.

Tufenkji, N., Ryan, J.N. and Elimelech, M., 2002. The promise of bank filtration. Environ. Sci. Technol., 36(21): 422A-428A.

Vasiliadou, I.A. and Chrysikopoulos, C.V., 2011. Cotransport of *Pseudomonas putida* and kaolinite particles through water-saturated columns packed with glass beads. Water Resour. Res., 47(2).

Verwey, E.J.W. and Overbeek, J.T.G., 1955. Theory of the stability of lyophobic colloids. J. Colloid Sci., 10(2): 224-225.

WHO, 2014. Preventing diarrhoea through better water, sanitation and hygiene. Exposures and impacts in low- and middle-income countries, Geneva, Switzerland.

Wu, Y. and Cheng, T., 2016. Stability of nTiO_2 particles and their attachment to sand: Effects of humic acid at different pH. Sci. Total Environ., 541: 579-589.

Xiao, Y. and Wiesner, M.R., 2013. Transport and retention of selected engineered nanoparticles by porous media in the presence of a biofilm. Environ. Sci. Technol., 47(5): 2246-2253.

Yao, K.-M., Habibian, M.T. and O'Melia, C.R., 1971. Water and waste water filtration. Concepts and applications. Environ. Sci. Technol., 5(11): 1105-1112.

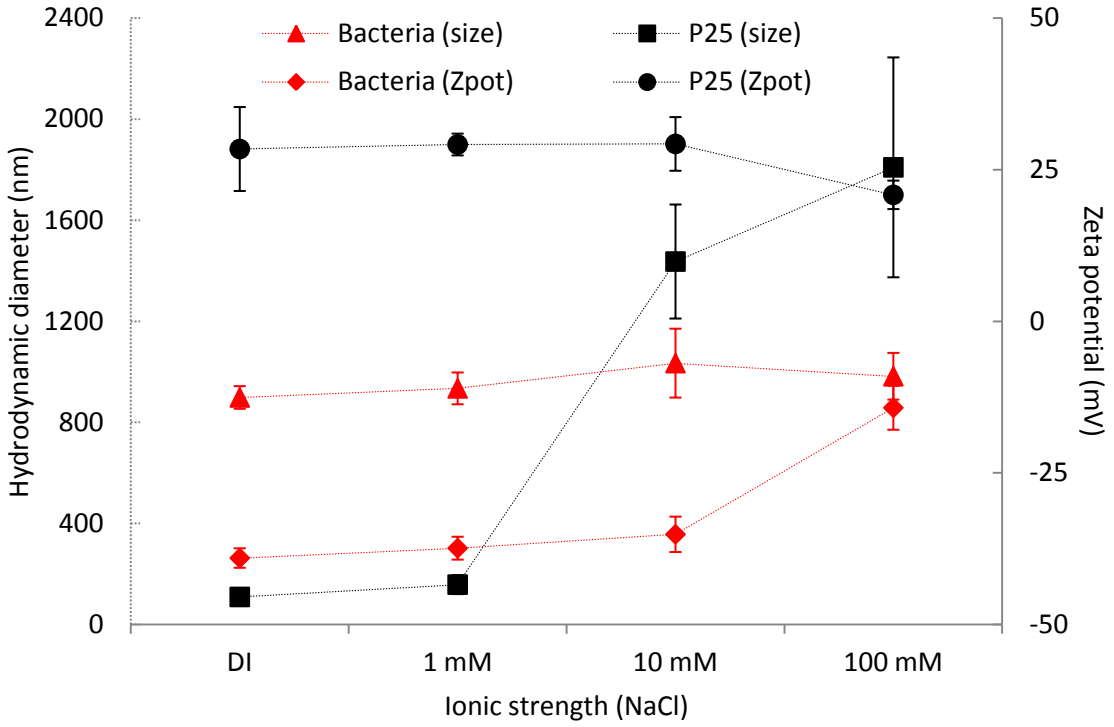

Fig. 1: Hydrodynamic diameter and zeta potential of bacteria and TiO_2 nanoparticles suspended in pure water (resistivity 18 MΩ.cm) and NaCl solutions; pH=5.8.

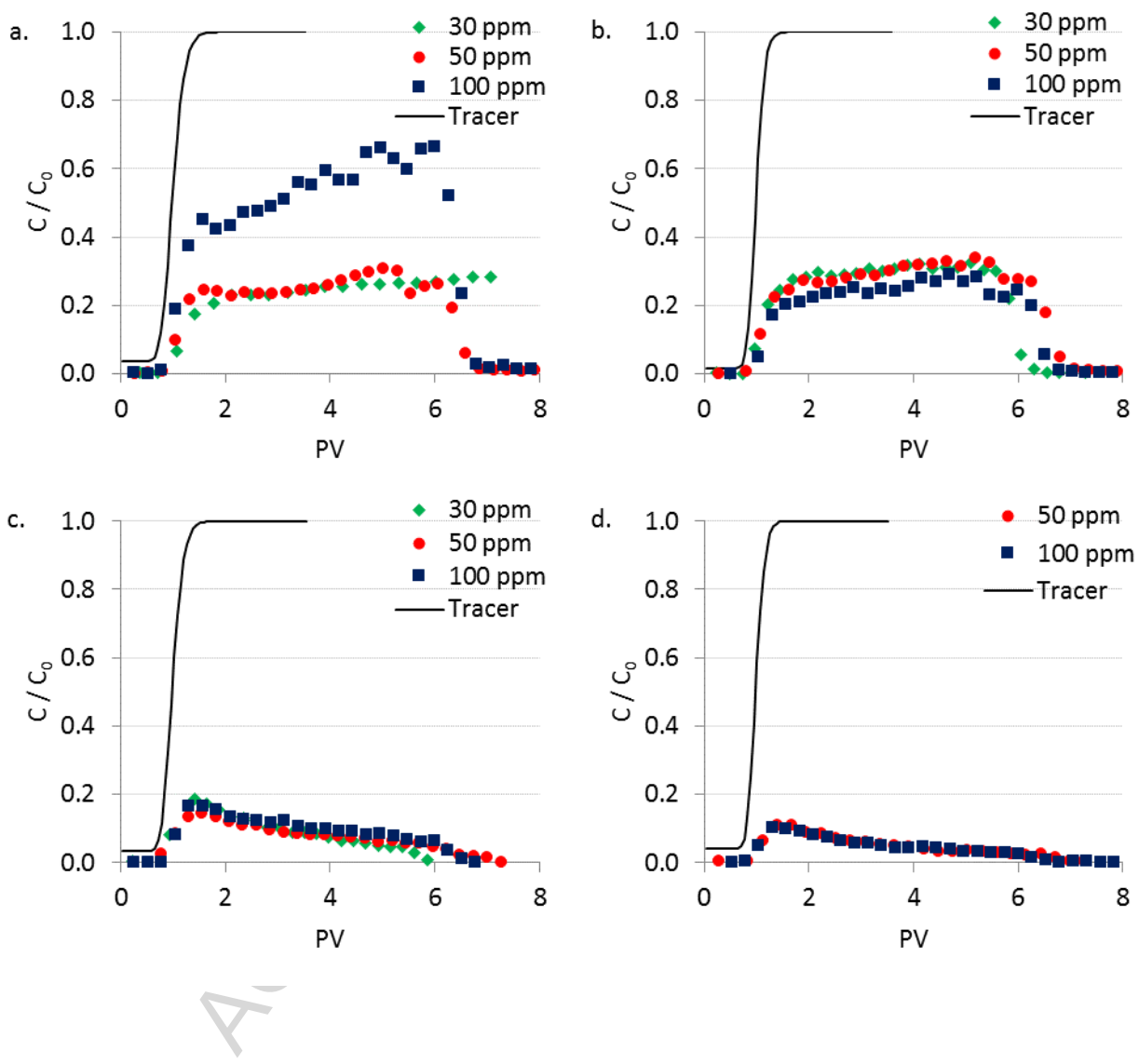

Fig. 2: Breakthrough curves for TiO_2 in sand columns suspended in different media: a. Ultrapure water (resistivity 18 MΩ.cm); b. 1 mM NaCl; c. 10 mM NaCl; d. 100 mM NaCl. pH=5.2-5.8.

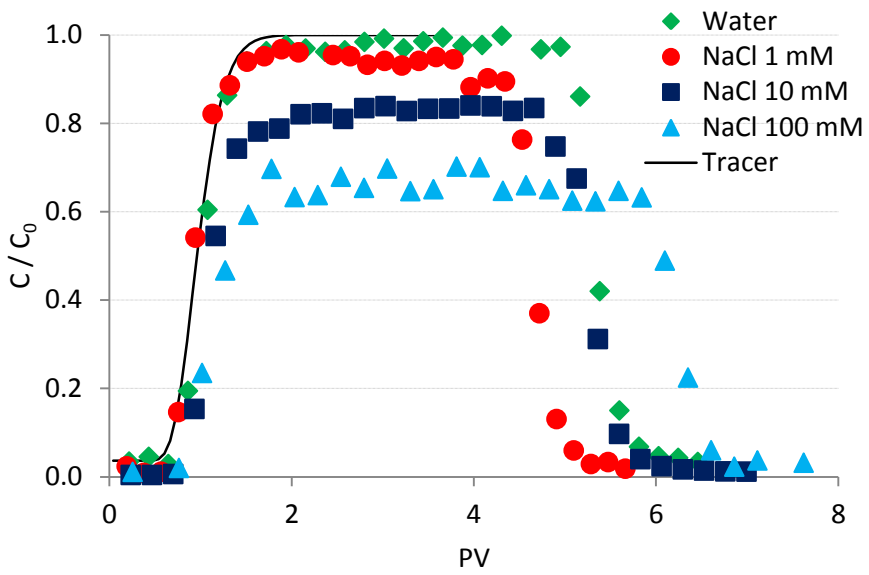

Fig. 3: Breakthrough curves for *Pseudomonas aeruginosa* in water (resistivity 18 MΩ.cm), NaCl 1 mM, 10 mM, 100 mM. pH=5.2-5.8.

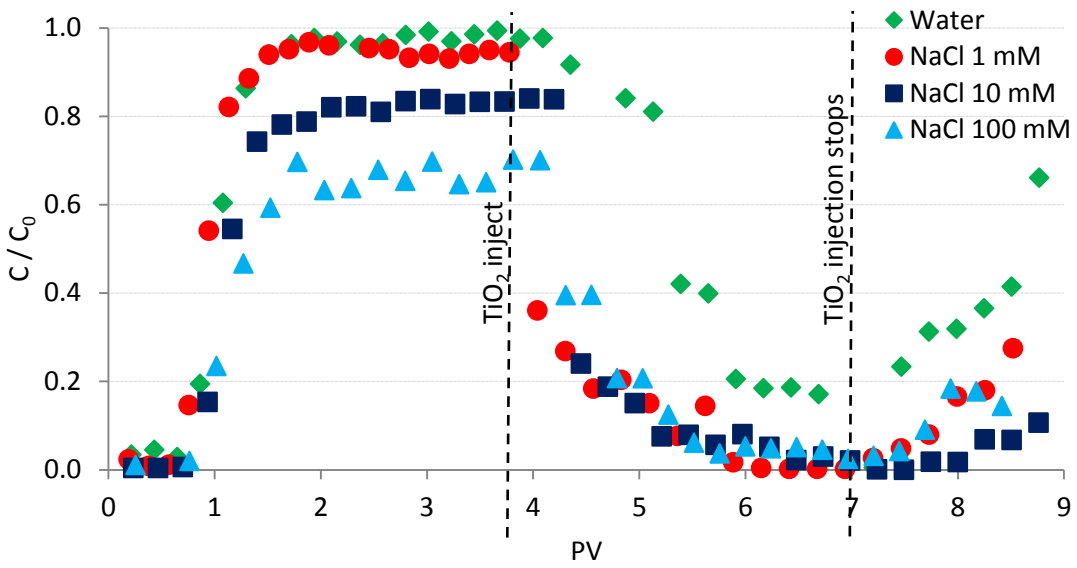

Fig. 4: Breakthrough curves for bacteria, measured by qPCR between 4 and 9 PV, in co-transport of bacteria and TiO_2.

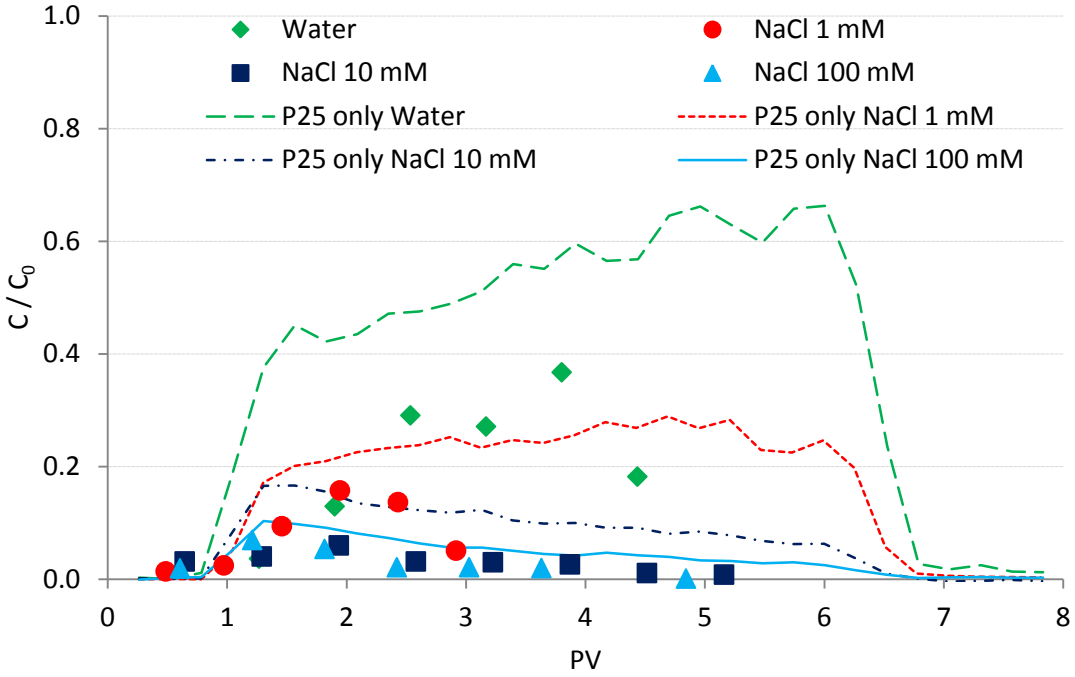

Fig. 5: Breakthrough curves for titanium measured by spectrophotometry at 410 nm after digestion and addition of H_2O_2 in co-transport of bacteria and TiO_2. Breakthrough curves for TiO_2 only for comparison.

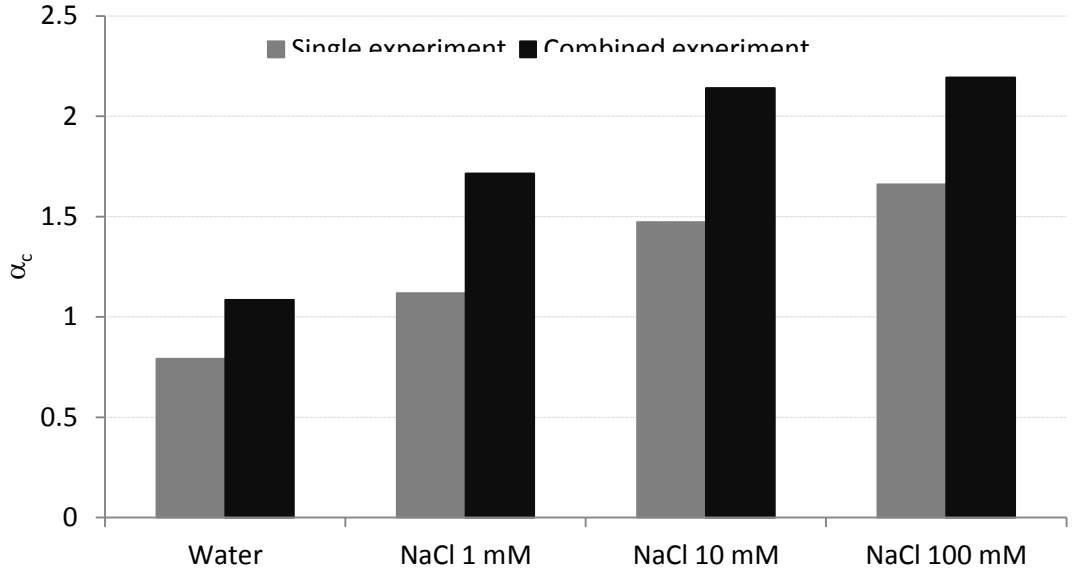

Fig. 6: Collision efficiency factor (α_c) for TiO_2 in the single experiment and pseudo-collision efficiency factor for TiO_2 in the combined experiment.

Table 1: Experimental conditions.

<table>
<tr><th></th><th>Ionic strength (mM NaCl)</th><th>Particle concentration</th><th>Detection method</th></tr>
<tr><td>Transport of TiO_2</td><td>0; 1; 10; 100</td><td>30; 50; 100 ppm</td><td>UV spec. (λ=325 nm)</td></tr>
<tr><td>Transport of P. aeruginosa</td><td>0; 1; 10; 100</td><td>5 mL stock bacteria + 95 mL solution</td><td>UV spec. (λ=262 nm)</td></tr>
<tr><td rowspan="5">Combined transport of TiO_2 and P. aeruginosa</td><td rowspan="5">0; 1; 10; 100</td><td>5 mL stock bacteria + 95 mL solution</td><td>UV spec. (λ=262 nm)</td></tr>
<tr><td colspan="2">followed by</td></tr>
<tr><td>5 mL stock bacteria + 95 mL solution with TiO_2 (50 ppm)</td><td>qPCR</td></tr>
<tr><td colspan="2">or</td></tr>
<tr><td>5 mL stock bacteria + 95 mL solution with TiO_2 (100 ppm)</td><td>Digestion + Vis. spec. (λ=410 nm)</td></tr>
</table>

Highlights

- Bacterial transport in groundwater was affected by the presence of nanomaterials. Retention of bacteria and TiO_2 nanoparticles in saturated sand beds was enhanced when both are present simultaneously in the suspensions.
- Heteroaggregation and electrostatic interactions controlled the deposition and retention in the cotransport experiments. Attachment of TiO_2 to the sand was explained by electrostatic forces and these nanoparticles acted as bond between bacteria and sand.
- DLVO and classical filtration theories were employed to model the interactions between particles and between particles and sand grains.